Solvent effects determine the sign of the charges of maximum entropy and capacitance at silver electrodes

Ravishankar Sundararaman[1, a)] and Kathleen Schwarz[2, b)]
[1)] *Department of Materials Science and Engineering, Rensselaer Polytechnic Institute, 110 8th St., Troy, New York 12180, United States*
[2)] *Material Measurement Laboratory, National Institute of Standards and Technology, 100 Bureau Dr., Gaithersburg, Maryland 20899, United States*

Fully harnessing electrochemical interfaces for reactions requires a detailed understanding of solvent effects in the electrochemical double layer. Predicting the significant impact of solvent on entropic and electronic properties of electrochemical interfaces has remained an open challenge of computational electrochemistry. Using molecular dynamics simulations of silver-water and silver-acetonitrile interfaces, we show that switching the solvent changes the signs for both the charges of maximum capacitance (CMC) and maximum entropy (CME). Contrasting the capacitance and CME behavior of these two interfaces, we demonstrate that the preferred orientation of the solvent molecule and the corresponding charge density determine the sign of the CMC and CME, and hence, the qualitatively-different charge asymmetry of the electrochemical interface.

The molecular structure of the electrochemical double layer plays a key role in catalysis by determining both the access of reaction species to the electrode and the subsequent reaction mechanisms.[1] Solvent molecules can block reactants, facilitate access to the electrode, or act as reactants in industrially-relevant electrochemical reactions such as the hydrogen evolution reaction, the oxygen reduction reaction, and the hydrogenation of acetonitrile for chemical manufacturing.[2] The molecular structure of the double layer changes as the electrode charges, changing the capacitance[3,4] and entropy.[5] We recently showed using molecular dynamics (MD) simulations of aqueous interfaces that both capacitance and entropy are asymmetric with electrode charge, with charges of maximum capacitance (CMC) and entropy (CME) both negative, but with distinct magnitudes.[6,7] However, the relationship between the molecular structure of the double layer and the charges of maximum capacitance and entropy is yet to be unraveled.

Here, we predict CMC and CME from MD simulations of Ag(100) interfaces with water and acetonitrile to identify the solvent effects on these quantities. We first compare MD simulations with explicit electrolyte against those with a pure-solvent + continuum electrolyte (i.e., an explicit solvent layer followed by region with solvent plus a continuum electrolyte), and observe only modest changes in both the CMC and CME, in agreement with small changes of the potential of maximum entropy with electrolyte in experiments.[8,9] In contrast, we find significant contributions to both the CMC and CME from the solvent, and find that their origins lie in the same molecular phenomenon. The molecular properties of the solvent determine the sign of the CMC and CME, with both flipping from negative for water to positive for acetonitrile.

Molecular dynamics simulations of an aqueous NaF - Ag(100) interface find that the electrochemical capacitance increases for negatively charged interfaces, reaching a maximum at a CMC of -3.7 μC/cm^2(Fig. 1(a)).[7] Here, we replace the explicit NaF electrolyte with a continuum electrolyte beyond an inner-layer width parameterized by z_2 (discussed below). Figure 1(a) shows that z_2 controls the overall magnitude of capacitance, but does not affect the shape of the capacitance curve, with the maximum remaining at a CMC of -3.1 μC/cm^2. The continuum electrolyte predictions for a physically-reasonable inner-layer width of $z_2 \approx 3$ Å closely match the explicit electrolyte predictions: the CMC is slightly smaller, but the peak shape and the most of the charge asymmetry is captured well. This indicates that the inner layer capacitance is determined by the solvent and is not modified substantially by the ions in a non-adsorbing electrolyte.[3]

Briefly, to predict electrochemical capacitance and entropy from pure-solvent MD simulations + continuum electrolyte, we apply an electric field to the solvent using charge densities $\pm\sigma$ on two electrodes in a simulation cell that is periodic in x, y and non-periodic in the z-direction (Fig. 1(b)). (See SI for further simulation details.) We then fit the linear electrostatic potential profile in the central bulk region to extract the field-dependent dielectric constant $\epsilon_b(\sigma)$ from the slope and the intercepts $\phi_{\rm int}(+\sigma)$ and $\phi_{\rm int}(-\sigma)$ on both electrodes (Fig. 1(c)), where $\sigma = D$, the externally applied electric field throughout the solvent region. From these quantities and the vacuum permittivity ϵ_0, we can reconstruct the effective inner layer potential $\phi_{\rm il}(\sigma) = \phi_{\rm int}(\sigma) - z_1\sigma/\epsilon_0 + z_2\sigma/(\epsilon_0\epsilon_b(\sigma))$, where z_1 accounts for the distance between the electrode atoms and its charge response plane (Δz in Ref. 6), while z_2 is the width of the solvent-only 'inner-layer' region of the electrochemical interface as in the Gouy-Chapman-Stern model. Note that we use the bulk permittivity $\epsilon_b(\sigma)$ only to define the interface potential $\phi_{\rm int}(\sigma)$, as a way of neatly separating bulk and interface contributions between these two charge dependent functions. The actual permittivity changes dramatically near the interface (where the potential oscillates in Fig. 1(c)) and is captured within $\phi_{\rm int}(\sigma)$ in our

[a)] Electronic mail: sundar@rpi.edu
[b)] Electronic mail: kas4@nist.gov

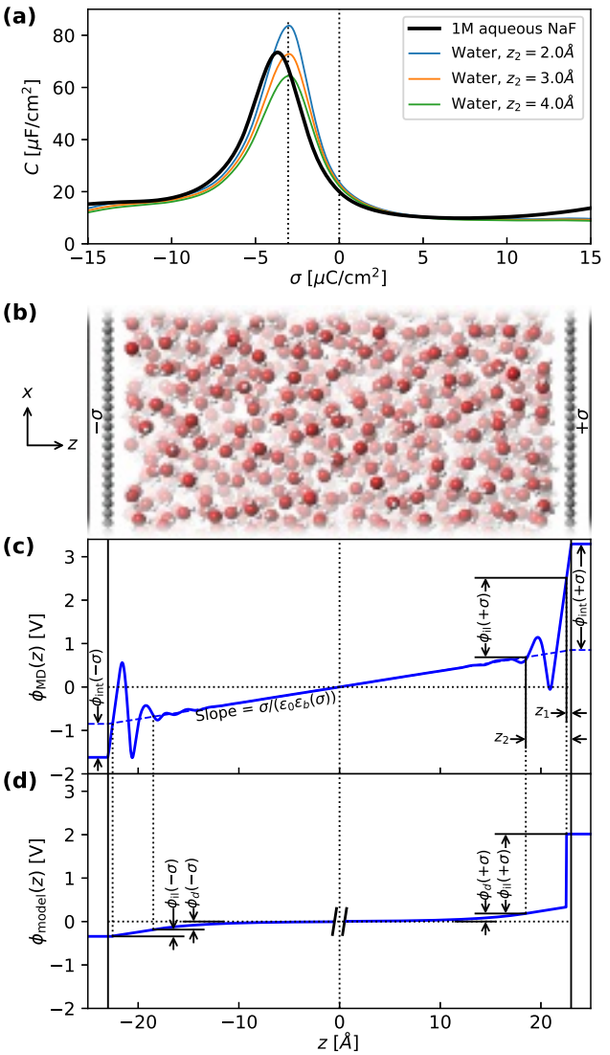

FIG. 1. (a) The charge-asymmetric capacitance from molecular dynamics simulations of 1 mol/liter aqueous NaF electrolyte interfaces[6,7] is closely matched by pure-solvent + continuum electrolyte beyond an inner-layer width $z_2 \approx 3$ Å, indicating that the solvent determines the sign of the charge asymmetry of the capacitance. (b) These predictions start from electrified pure-solvent interface simulations, and (c) use the electrostatic potential profile, $\phi_{\rm MD}(z)$, to extract field-dependent dielectric constant $\epsilon_b(\sigma)$ and intercept $\phi_{\rm int}(\sigma)$. The inner layer potential $\phi_{\rm il}(\sigma)$ accounting for electrode charge response location z_1 and inner-layer width z_2 is (d) combined with Debye-model diffuse layer potential $\phi_d(\sigma)$ to predict the overall half-cell potential profiles, $\phi_{\rm model}(z)$, and electrochemical capacitance.

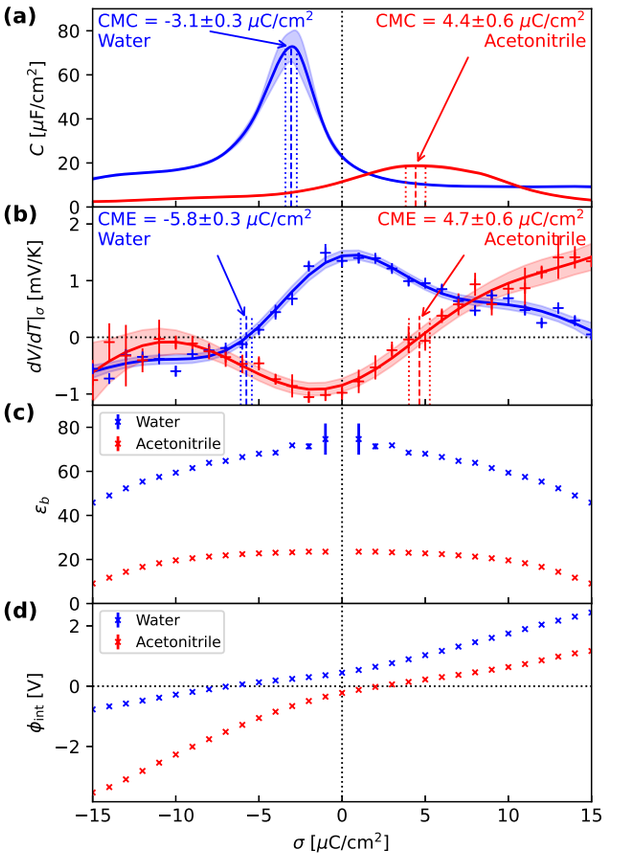

FIG. 2. (a) Water and acetonitrile exhibit opposite charge asymmetry in capacitance, with charge of maximum capacitance (CMC) negative for water and positive for acetonitrile. (b) The charge of maximum entropy (CME), located by the zero crossing of dV/dT, is also negative for water and positive for acetonitrile. The CME and CMC are distinct for water, but comparable within error bars for acetonitrile. The above results are based on a pure-solvent inner layer combined with a 1 mol/liter continuum electrolyte diffuse layer. (c) The field-dependent dielectric constant is symmetric by definition, and all asymmetry in the inner layer potential leading to the CMC and CME arises from (d) the intercept potential $\phi_{\rm int}(\sigma)$ (see Fig. 1(c) for definition).

approach. Finally, we calculate the overall potential in the electrochemical interface as $\phi(\sigma) = \phi_{\rm il}(\sigma) + \phi_d(\sigma)$, where $\phi_d(\sigma)$ is the potential across the diffuse layer at a specified ionic concentration from the Debye model (see SI), effectively constructing the potential of the half-cells shown in Fig. 1(d), and predict the differential capacitance $C(\sigma) = d\phi(\sigma)/d\sigma$. This allows us to predict the overall capacitance of ideal electrochemical interfaces for different ionic concentrations starting from a single set of pure-solvent MD simulations. As discussed above, we find that $z_2 = 3$ Å of solvent, plus continuum electrolyte, reasonably captures the explicit 1 mol/liter electrolyte predictions, while the electrode-plane distance $z_1 = 0.46$ Å remains unchanged from the explicit electrolyte simulations.[6,7]

Now that we have shown that solvent MD + continuum electrolyte closely approximates explicit electrolyte MD simulations with $z_1 = 0.46$ Å and $z_2 = 3.0$ Å, we fix these parameters as well as the continuum elec-

trolyte concentration of 1 mol/liter and investigate the solvent dependence. Figure 2(a) shows that water and acetonitrile exhibit opposite asymmetry in the capacitance, with charges of maximum capacitance (CMC) of (-3.1 ± 0.3) μC/cm^{2}and $(+4.4 \pm 0.6)$ μC/cm^2 respectively. Next, to predict asymmetry in the entropy of the interface, we simulate heating of the interfaces, directly mimicking experimental measurements of the charge of maximum entropy (CME).[10] Specifically, from the thermodynamic relation $\partial S/\partial\sigma|_T = -\partial V/\partial T|_\sigma$, where V is the interface potential difference, the maximum of entropy $S(\sigma)$ occurs where $\partial V/\partial T|_\sigma$ crosses 0 with a positive slope. From the $\partial V/\partial T|_\sigma$ shown in Figure 2(b), computed from a finite difference of MD simulations at 298 K and 318 K,[6] we see that water and acetonitrile also exhibit opposite asymmetry in entropy with CMEs of (-5.8 ± 0.3) μC/cm^{2}and $(+4.7 \pm 0.6)$ μC/cm^2 respectively. The uncertainty in the capacitance (shaded regions in these figures), and hence in the CMC and CME, are calculated by resampling from five independent MD simulations at each charge, as discussed in Ref. 6. Note that the sign of the CMC and CME are identical for each solvent. Their magnitudes differ for water, but for agree within the uncertainties for acetonitrile.

To break down the contributions to the capacitance and entropy predictions, Figure 2(c) and (d) respectively show the bulk dielectric constant ϵ_b from the slope and the intercept ϕ_{int} of the MD electrostatic potential profiles (defined in Figure 1(c)). The bulk dielectric constant decreases symmetrically with increasing charge magnitude, due to dielectric saturation with the applied electric field $E = \sigma/\epsilon_0$. This saturation is captured well by the Booth equation for bulk water and acetonitrile,[11,12] and is relevant for electrochemical interfaces with ϵ_b reducing by more than a factor of 2 over the range of relevant electrode charges.[13] This bulk ϵ_b is relevant in determining the diffuse-layer and hence the total capacitance, but is distinct from the changes in the interface dielectric constant. These changes are captured within ϕ_{int}, which encapsulates all interfacial contributions in the present approach. Since ϵ_b is symmetric by definition, all the asymmetry in the capacitance and entropy is necessarily from the intercept potential, ϕ_{int}. Note that the ϕ_{int} at zero charge has opposite signs for water and acetonitrile, increases monotonically with charge and crosses zero at negative and positive signs respectively. However, the zero-crossing of ϕ_{int} is not directly connected to CMC or CME; the capacitance contribution from the interface is related to the second charge derivative $\partial^2\phi_{\text{int}}/\partial\sigma^2$, while the entropy contribution is related to the temperature derivative $\partial\phi_{\text{int}}/\partial T$.

To connect CMC and CME to the molecular behavior of the solvent at the interface, Figure 3 compares the solvent charge density distribution and its temperature derivative at the interface for various electrode charges. Note that the solvent response is expected to dominate the overall charge response in the inner-layer region shown here, an idealized interface of a silver electrode and weakly interacting, non-adsorbing electrolyte. The charge density of water closest to the electrode is positive at zero electrode charge (gray line in Figure 3(a)), indicating an interfacial water orientation with the hydrogen slightly closer to the electrode on average. This slight charge imbalance, with a small positive (negative) charge density near (away from) the electrode is consistent with experimental predictions of water molecules in a flat orientation at neutral silver-water interfaces.[14,15] This charge density increases in magnitude for negative electrode charges, but for positive electrode charges, decreases in magnitude first, then crosses zero (near $\sigma = 8$ μC/cm^2) and finally increases in magnitude with oxygen now facing the electrode. Additionally, the location of the charge density is much closer to the electrode when the hydrogen faces the negative electrode,

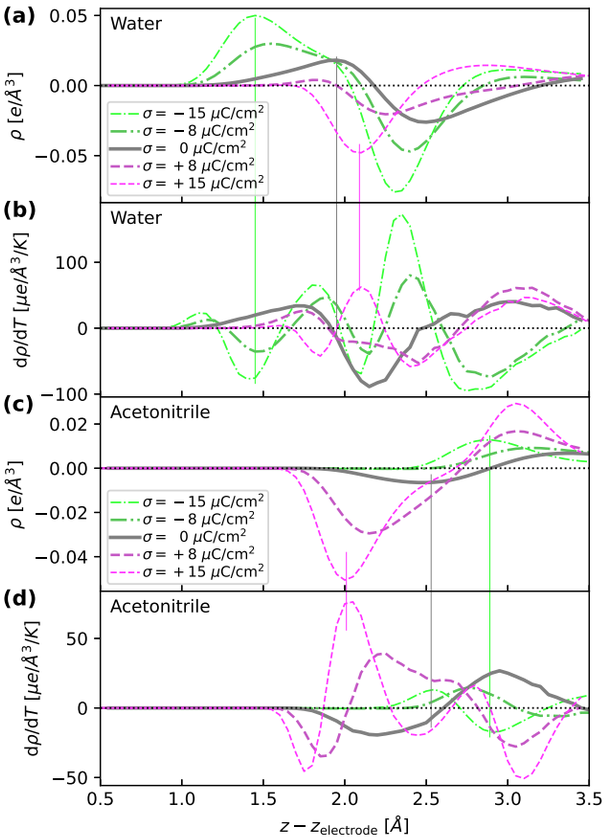

FIG. 3. Spatial distribution of solvent charge density ρ and its temperature derivative for (a, b) water and (c, d) acetonitrile, near electrodes with varying surface charge densities σ. The peak of ρ closest to the neutral electrode is positive for water and negative for acetonitrile, and this peak moves closer to the electrode with increasing temperature, leading to the same behavior for the closest peak of $d\rho/dT$. This common molecular orientation preference of the solvent at the interface, H-facing for water and CN-facing for acetonitrile, lead to a common sign for CMC and CME (opposite between solvents), but with different magnitudes in general.

compared to when the oxygen is next to the positive electrode. This molecular behavior leads to a stronger solvent response to negative charges, leading to a negative CMC, as discussed previously.[6]

The above behavior is reversed overall from water to acetonitrile. The solvent charge nearest the neutral electrode (gray line in Figure 3(c)) is negative, indicating the CN end of the molecule facing the electrode. For large enough magnitude of $\sigma < 0$, this charge density flips positive, with CH_3 facing the electrode. This behavior is in agreement with Sum Frequency Generation (SFG) measurements on Pt electrodes, where acetonitrile binds strongly,[16] and reversibly flips between CH_3 and CN towards the metal at low and high potentials respectively.[17] For acetonitrile, the negative (CN) solvent charge approaches the positively charged electrodes more closely than the positive (CH_3) solvent charge approaches the negative electrodes, leading to stronger charge response for $\sigma > 0$ and hence a positive CMC. Thus, the opposite sign of CMC for water and acetonitrile stems from the closer electrode approach of the positive H end of water and negative CN end of acetonitrile, compared to the negative O and positive CH_3 ends respectively.

To understand the entropy response and CME, we need to compare the behavior of ρ and $d\rho/dT$ for both solvents. To relate the charge of maximum entropy to the molecular interaction at the interface, we first consider the neutral interface. For the neutral interfaces of both water and acetonitrile, the peaks of ρ closest to the electrode in Figure 3(a, c) line up with the zero crossings of $d\rho/dT$ in Figure 3(b, d) (connected by grey vertical lines). This signature, along with the direction of zero crossing, corresponds to a charge density that moves closer to the electrode with increasing temperature. This is expected from a thermodynamic standpoint: as the temperature increases, more thermal energy is available to overcome the repulsive potential at the interface. In contrast, for the highly charged electrodes with $\sigma = \pm 15\ \mu C/cm^2$, the peaks of ρ line up with opposite peaks of $d\rho/dT$ (green and magenta vertical lines), which indicates that the ρ peak primarily broadens with increasing temperature. The commonality of these behaviors lead to the sign of ρ and $d\rho/dT$ nearest the interface being linked. This leads to the CMC and CME having the same sign in general, as they stem from the same molecular orientation preferences, but they could differ in magnitude as that depends on further details of the overall complex charge distributions and temperature derivatives in Figure 3.

Finally, to aid direct experimental comparisons, Figure 4 plots the simulated capacitance as a function of electrode potential (instead of electrode charge in previous figures). Additionally, we present results for several ionic concentrations in the diffuse capacitance contribution, approximated using the Gouy Chapman model (essentially the nonlinear Poisson-Boltzmann model). For both water and acetonitrile, the capacitance drop is centered at the potential of zero charge when the ionic concentration is sufficiently low, irrespective of the asymmetry of the solvent response which affects the shape of the capacitance curves at larger magnitudes of potential. However, the capacitance curves for both water[18] and acetonitrile appear to be narrower than those observed experimentally.

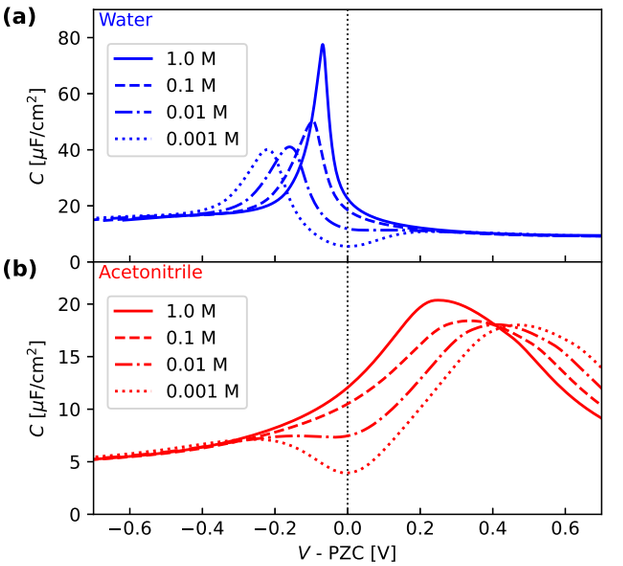

FIG. 4. Capacitance as a function of ionic concentration by combining a modified Poisson-Boltzmann model of the electrolyte with the inner layer potential from molecular dynamics simulations for (a) water and (b) acetonitrile. Low diffuse layer capacitance of the neutral electrode leads to a dip in the capacitance for low ionic concentrations centered at the potential of zero charge, independent of the asymmetry in the capacitance introduced by the solvent.

This underestimated width of the capacitance curves may be caused by missing chemisorption interactions in our simulation. Specifically, a classical force field may not be able to adequately represent the intrinsically quantum-mechanical strong attraction of the water to the metal interface, beyond the average metal-molecule interactions captured by parameterizing the wall interaction to DFT (see SI). AIMD simulations of the aqueous double layer of Pt(111)[19] suggest that chemisorption of water onto the electrode surface leads to the experimentally observed bell-shaped capacitance feature.[20] The chemisorption of water to silver interfaces is believed to be weaker than that of platinum, but the electronic interaction is still strong enough to significantly shift the potential of zero charge (PZC) away from its expected value based on the work function,[21] and so may still play an important role in determining the capacitance. Note however that the ab initio molecular dynamics simulations are typically coupled with a capacitance model for the bulk solvent that is constant with potential,[19] and thus may not adequately describe the solvent contributions to the capacitance that are captured by the longer and larger classical MD simulations presented here.

For acetonitrile, we note that qualitatively the Ag-acetonitrile interface for both NaF and $LiClO_4$ electrolyte has increasing capacitance with potential across the potential of zero charge[22,23]. A more quantitative comparison of the capacitance curve width is difficult for acetonitrile because of the experimental challenges with the chemical stability of the interface, including oxidation of the surface and contamination by solvent impurities.[22,23]

In conclusion, we related the CMC and CME to the molecular behavior of the solvent, and compared the opposite-charged behavior of the silver interface with acetonitrile and water. Continuum treatment of ions does not significantly change the CMC or CME compared to explicit MD simulations of ions, allowing us to systematically investigate solvent effects in water and acetonitrile, and setting the stage for expanding this analysis to several more solvents in future work. The natural orientation of solvent molecules at the neutral electrode leads to closer charge approach to electrodes of one charge sign compared to the other, which leads directly to the common sign of the CMC and CME. The overall shape of capacitance from these classical MD simulations does not match experiment perfectly, likely due to missing solvent chemisorption. Future work is needed to combine such effects captured naturally in AIMD with the longer sampling times and larger bulk regions captured in our classical MD simulations. This includes extending the present approach to pure-solvent AIMD + continuum electrolyte as a strategy to reduce the required time scales.[24] Combinations of electronic DFT with classical MD,[25] AIMD simulations and the detailed solvent response models developed here hold promise for a more complete picture of electrified electrochemical interfaces.

SUPPLEMENTARY MATERIALS

See supplementary information for details of the molecular dynamics simulations in the LAMMPS,[26] including force field details for water (SPC/E)[27] and acetonitrile,[28] parametrization of silver-solvent interactions from electronic density functional theory calculations in JDFTx,[29] and input files and analysis scripts for all results presented above.

Note: Certain software are identified in this paper to foster understanding. Such identification does not imply recommendation or endorsement by the National Institute of Standards and Technology, nor does it imply that the software identified is necessarily the best available for the purpose.

ACKNOWLEDGEMENTS

RS acknowledges support from the U.S. Department of Energy, Office of Science, Basic Energy Sciences, under Award #DE-SC0022247. Calculations were carried out at the Center for Computational Innovations at Rensselaer Polytechnic Institute, at NIST and at the National Energy Research Scientific Computing Center (NERSC), a U.S. Department of Energy Office of Science User Facility located at Lawrence Berkeley National Laboratory, operated under Contract No. DE-AC02-05CH11231 using NERSC award ERCAP0020105.

REFERENCES

[1] M. Yan, Y. Kawamata, and P. S. Baran, Chem. Rev. **117**, 13230 (2017).
[2] R. Xia, D. Tian, S. Kattel, B. Hasa, H. Shin, X. Ma, J. G. Chen, and F. Jiao, Nat. Commun. , 1949 (2021).
[3] S. Park and J. G. McDaniel, J. Phys. Chem. C **126**, 16461 (2022).
[4] M. H. Motevaselian and N. R. Aluru, ACS Nano **14**, 12761 (2020).
[5] J. A. Harrison, J. E. B. Randles, and D. J. Schiffrin, J. Electroanal. Chem. Interfacial Electrochem. **48**, 359 (1973).
[6] A. Shandilya, K. Schwarz, and R. Sundararaman, J. Chem. Phys. **156**, 014705 (2022).
[7] A. Shandilya, K. Schwarz, and R. Sundararaman, J. Chem. Phys. **156**, 129901 (2022).
[8] R. W. Haid, X. Ding, T. K. Sarpey, A. S. Bandarenka, and B. Garlyyev, Curr. Opin. Electrochem. **32**, 100882 (2022).
[9] X. Ding, D. Scieszka, S. Watzele, S. Xue, B. Garlyyev, R. W. Haid, and A. S. Bandarenka, ChemElectroChem **9**, e202101088 (2022).
[10] V. Climent, B. A. Coles, and R. G. Compton, J. Phys. Chem. B **106**, 5258 (2002).
[11] I. N. Daniels, Z. Wang, and B. B. Laird, J. Phys. Chem. C **121**, 1025–1031 (2017).
[12] F. Booth, J. Chem. Phys. **19**, 391 (1951).
[13] K. Schwarz and R. Sundararaman, Surf. Sci. Rep. **75**, 100492 (2020).
[14] Z. D. Schultz, S. K. Shaw, and A. A. Gewirth, J. Am. Chem. Soc. **127**, 15916 (2005).
[15] K. Ataka, T. Yotsuyanagi, and M. Osawa, J. Phys. Chem. **100**, 10664–10672 (1996).
[16] O. Petrii and I. Khomchenko, J. Electroanal. Chem. Interf. Electrochem. **106**, 277 (1980).
[17] S. Baldelli, G. Mailhot, P. Ross, Y.-R. Shen, and G. A. Somorjai, J. Phys. Chem. B **105**, 654 (2001).
[18] G. Valette, J. Electroanal. Chem. Interf. Electrochem. **138**, 37 (1982).
[19] J.-B. Le, Q.-Y. Fan, J.-Q. Li, and J. Cheng, Sci. Adv. **6**, 10.1126/sciadv.abb1219 (2020).
[20] K. Ojha, K. Doblhoff-Dier, and M. T. M. Koper, Proc. Natl. Acad. Sci. **119**, e21160161 (2021).
[21] J. Le, M. Iannuzzi, A. Cuesta, and J. Cheng, Phys. Rev. Lett. **119**, 016801 (2017).
[22] V. Safonov, M. Choba, and O. Petrii, J. Electroanal. Chem. **808**, 278 (2018).
[23] V. Safonov, A. Krivenko, and M. Choba, Electrochim. Acta **53**, 4859–4866 (2008).
[24] R. Sundararaman, D. Vigil-Fowler, and K. Schwarz, Chem. Rev. **122**, 10651 (2022).
[25] S.-J. Shin, D. H. Kim, G. Bae, S. Ringe, H. Choi, H.-K. Lim, C. H. Choi, and H. Kim, Nat. Comm. **13**, https://doi.org/10.1038/s41467-021-27909-x (2022).
[26] S. Plimpton, J. Comput. Phys. **117**, 1 (1995).
[27] H. J. Berendsen, J. R. Grigera, and T. P. Straatsma, J. Phys. Chem. **91**, 6269 (1987).
[28] V. A. Koverga, O. M. Korsun, O. N. Kalugin, B. A. Marekha, and A. Idrissi, J. Mol. Liq. **233**, 251 (2017).
[29] R. Sundararaman, K. Letchworth-Weaver, K. A. Schwarz, D. Gunceler, Y. Ozhabes, and T. Arias, SoftwareX **6**, 278 (2017).

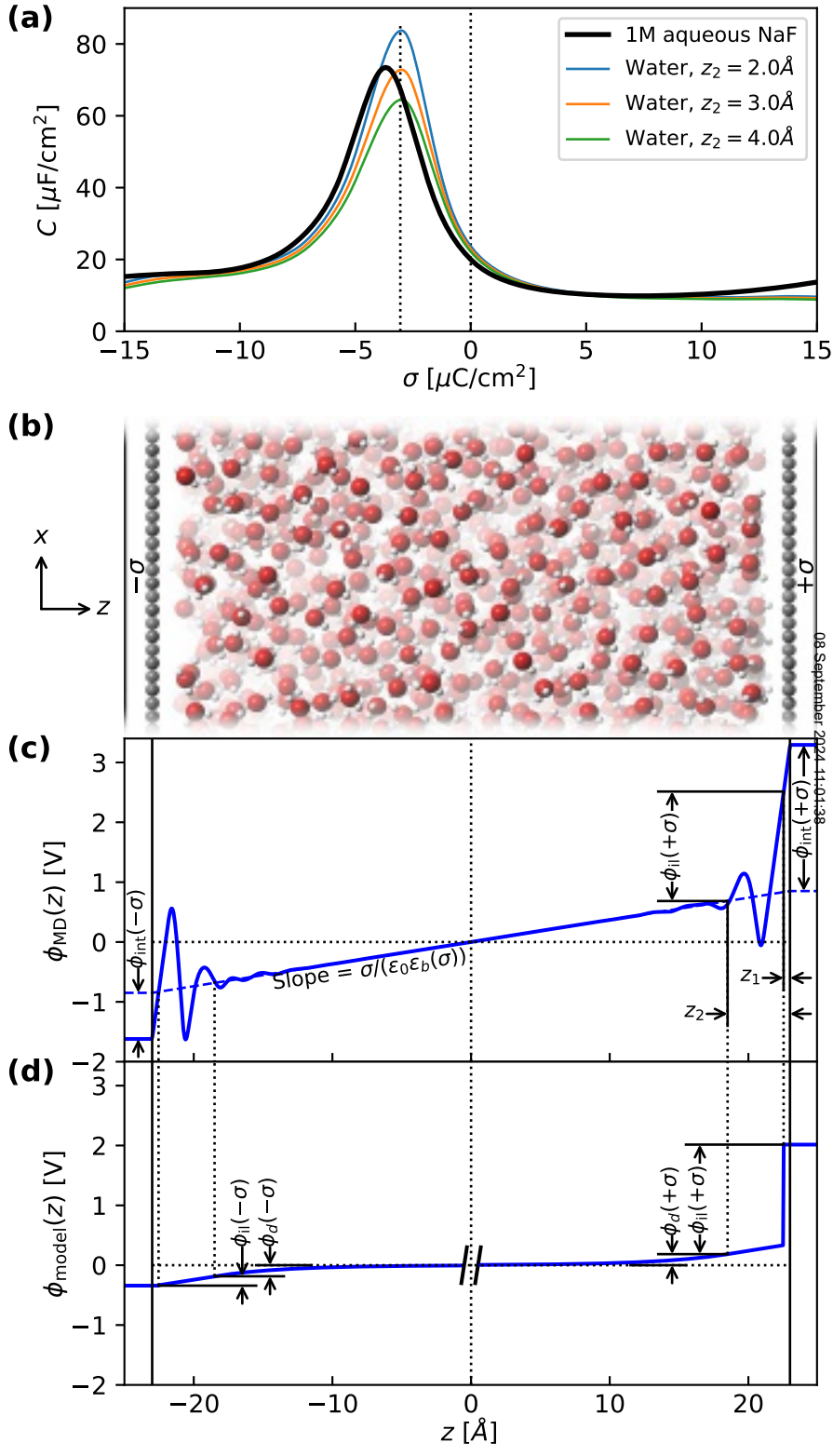

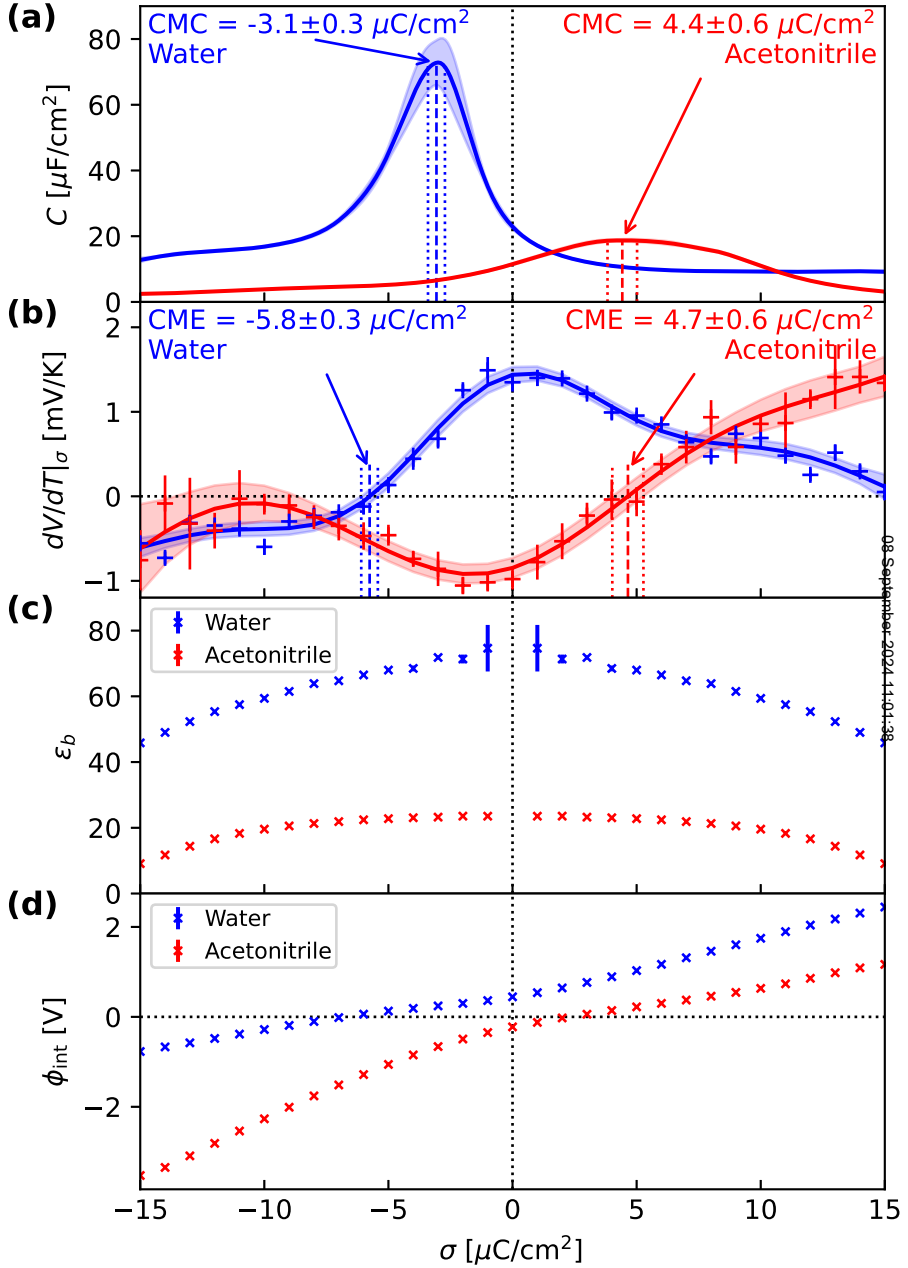
(a)
CMC = -3.1±0.3 μC/cm²
Water
CMC = 4.4±0.6 μC/cm²
Acetonitrile
C [μF/cm²]
(b)
CME = -5.8±0.3 μC/cm²
Water
CME = 4.7±0.6 μC/cm²
Acetonitrile
dV/dT|σ [mV/K]
(c)
Water
Acetonitrile
εb
(d)
Water
Acetonitrile
ϕint [V]
σ [μC/cm²]
08 September 2024 11:01:38

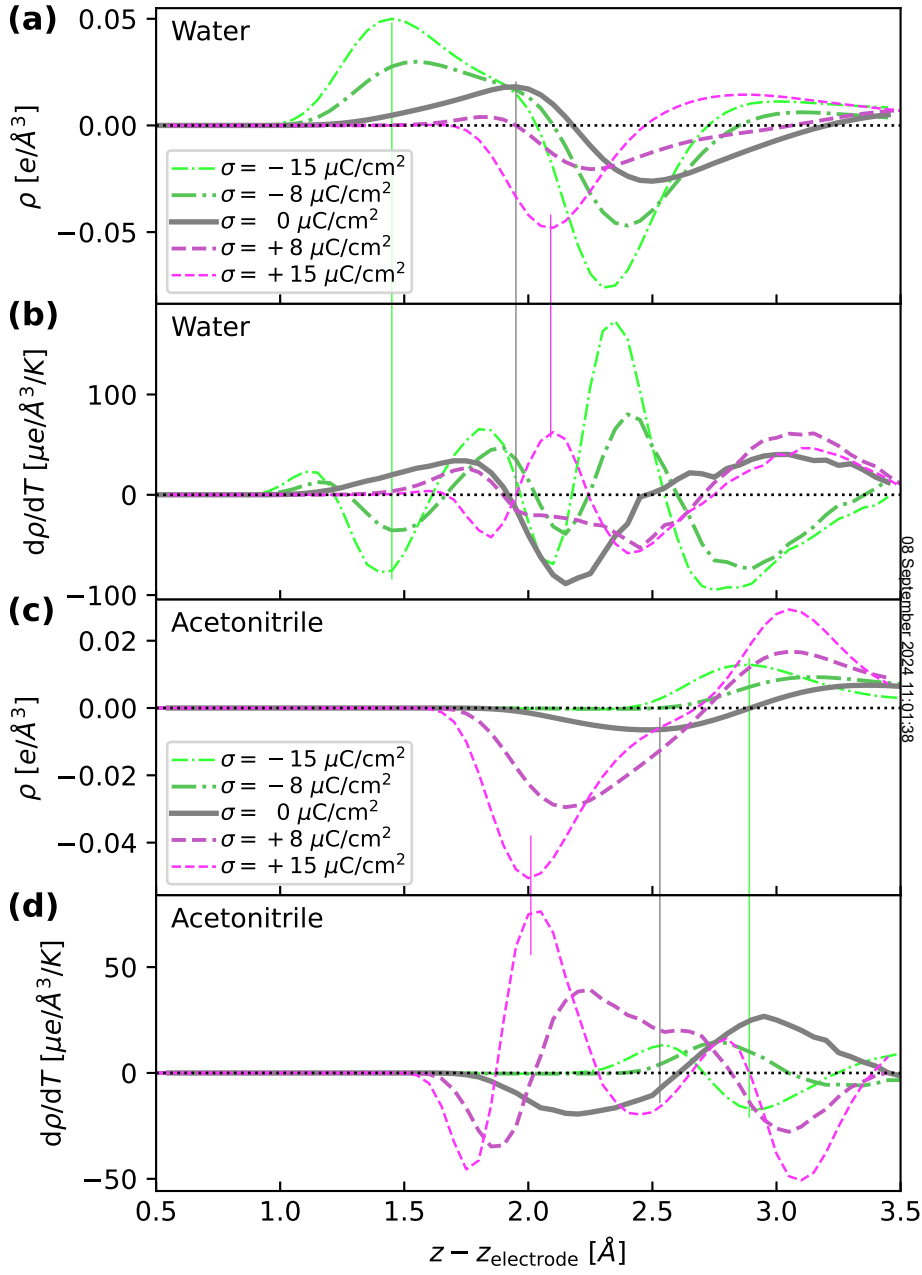
(a)
Water
ρ [e/Å³]
0.05
0.00
−0.05
σ = −15 μC/cm²
σ = −8 μC/cm²
σ = 0 μC/cm²
σ = +8 μC/cm²
σ = +15 μC/cm²
(b)
Water
dρ/dT [μe/Å³/K]
100
0
−100
(c)
Acetonitrile
ρ [e/Å³]
0.02
0.00
−0.02
−0.04
(d)
Acetonitrile
dρ/dT [μe/Å³/K]
50
0
−50
0.5
1.0
1.5
2.0
2.5
3.0
3.5
z − z_electrode [Å]
08 September 2024 11:01:38

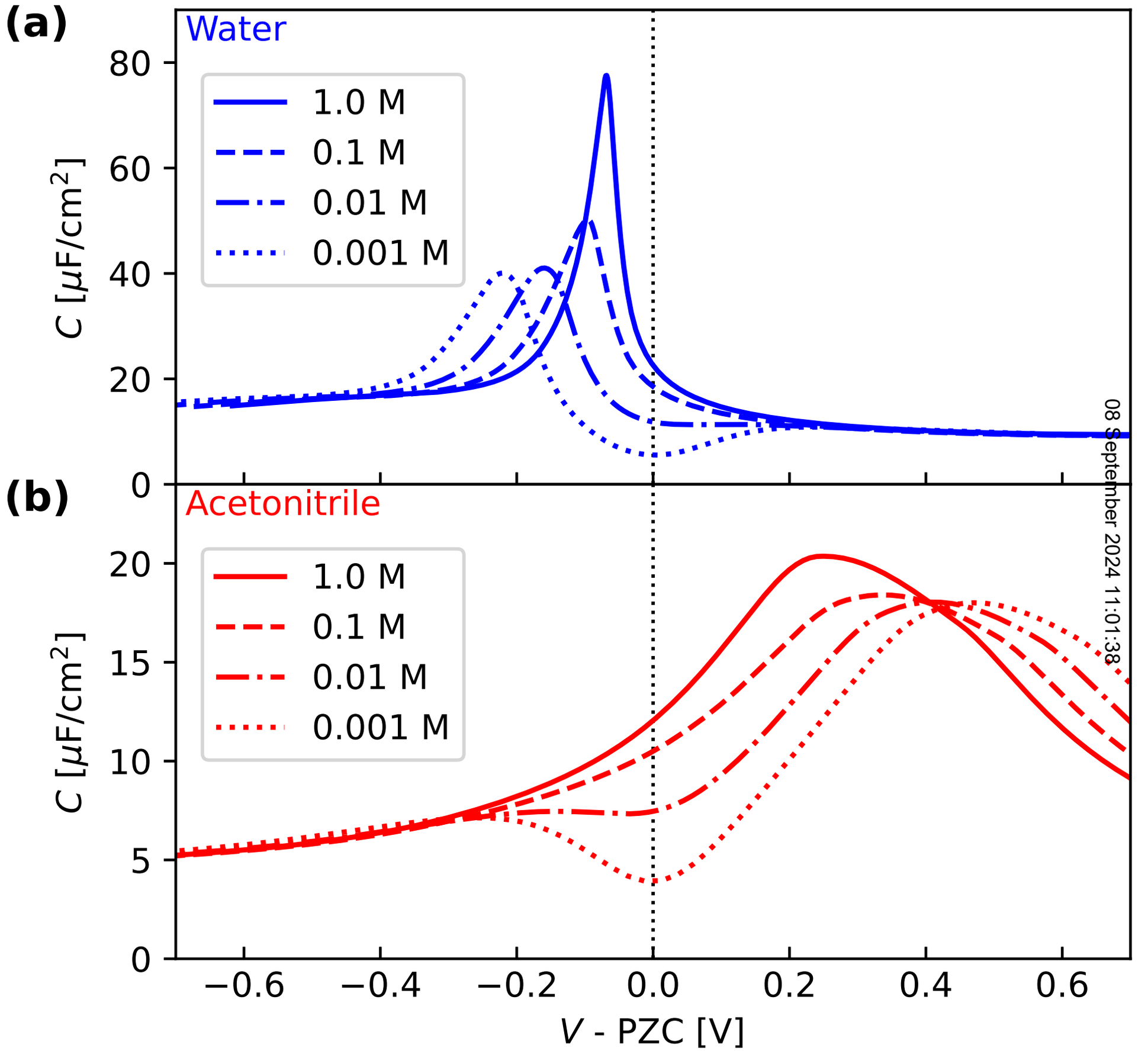
(a)
Water
1.0 M
0.1 M
0.01 M
0.001 M
C [μF/cm²]
80
60
40
20
0
(b)
Acetonitrile
1.0 M
0.1 M
0.01 M
0.001 M
C [μF/cm²]
20
15
10
5
0
−0.6
−0.4
−0.2
0.0
0.2
0.4
0.6
V - PZC [V]
08 September 2024 11:01:38